Geomorphic assessment of Tsäl̄njik Chú (Nordenskiold River) near Carmacks, Klondike region, Yukon

Carolyn Hatton*
Harquail School of Earth Sciences, Laurentian University

Alessandro Ielpi
Department of Earth, Environmental and Geographic Sciences, University of British Columbia
Vale Living with Lakes Centre, Laurentian University

Derek C. Cronmiller and Moya Painter
Yukon Geological Survey

Hatton, C., Ielpi, A., Cronmiller, D.C. and Painter, M., 2023. Geomorphic assessment of Tsäl̄njik Chú (Nordenskiold River) near Carmacks, Klondike region, Yukon. *In:* Yukon Exploration and Geology 2022, K.E. MacFarlane (ed.), Yukon Geological Survey, p. 77–91.

Abstract

River course migration is controlled by discharge, sediment supply, and bank vegetation, and its study informs watershed responses to environmental stressors like climate change and permafrost thaw. We present a preliminary characterization of Tsäl̄njik Chú (Nordenskiold River) near Carmacks (Klondike region, Yukon), based on geomorphic observations, time-series photogrammetry and hydrological analysis. We report channel-migration data in relation to flooding patterns, including the records of a recent ~10-year recurrence flood that took place in the spring of 2022. Boreholes drilled in the river's floodplain have encountered discontinuous permafrost at depths of >0.7 m, and preliminary morphodynamic analyses show similar relationships between channel size, curvature and migration rate to rivers outside the permafrost zone. Results provide a coarse characterization of hazards related to bank erosion and channel overspill at Carmacks, and will inform future work that integrates aspects of fluvial morphodynamics and biogeochemistry in relation to flooding elsewhere in Yukon.

* chatton@laurentian.ca

Introduction

Meandering rivers are ubiquitous fluvial landforms in the intermountain lowland plains of western and northern Canada (Nanson, 1980; Nanson and Hickin, 1983), and are characterized by a low-gradient (~0.01%) mainstem with anabranching side-channels. These rivers are characterized by planform whereby horseshoe-shaped bends (meanders) with opposite sense of curvature are found in sequence. Each meander is sided by an inner and an outer bank, which are characterized, in turn, by predominantly depositional and erosional processes (Jackson, 1976) constitute the bulk of surficial point-bar sediment in very sharply curved bends and in gently curved bends, and can be preserved preferentially by common types of bend migration. Preservation of the depositional facies of each meander bend depends upon the type of deformation (migration). In actively migrating meanders, erosional processes related to the inertia of the channel flow erode soil, vegetation and underlying sediment from outer banks. Eroded materials are variably redistributed over variable length-scales along inner banks, which grow over time into sediment accumulations with curved planform known as point bars. Concurrent depositional and erosional processes along the banks result in an outwards, lateral migration of the river channel; notably, outer bank erosion is matched by inner bank deposition over decadal to centennial timescales, such that the channel maintains constant width (Mason and Mohrig, 2019). Continued migration of meanders can lead to two bends intersecting each other and isolating a channel section in between (neck cutoff); alternatively, the growth of meanders is at times interrupted by cross-bar channels carved during exceptional floods (chute cutoff; Lewis and Lewin, 1983; Constantine and Dunne, 2008).

Processes of fluvial deposition and erosion, including those that lead to meander migration, take place at rates that are nonlinearly controlled by a multitude of factors, some of which are intrinsic (e.g., the curvature of a channel bend) and other extrinsic (e.g., water discharge and sediment supply; Donovan et *al.*, 2021). Discharge and sediment availability are, in turn, dependent on the hydro-climatic, geological and geomorphological context of a region. As such, river morphodynamics are affected, over certain spatial and temporal scales, by environmental changes in such things as precipitation, temperature or land-use (Horton et *al.*, 2017). The western Canadian Arctic is one such region where ecosystems are impacted by climate change (e.g., increasing temperature and precipitation). Compared to localities in Canada's southern provinces, the mean temperature increase over the past several decades has nearly doubled in some arctic areas (Gillet et *al.*, 2019), and northern regions such as Yukon are currently experiencing among the sharpest warming trends on Earth. Trends in temperature and precipitation affect flood magnitude and frequency and, by extension, impact infrastructures and communities located along riverbanks that may depend on waterways for seasonal transportation or traditional food harvesting.

This report deals with Tsāl̄njik Chú, also known as the Nordenskiold River, upstream of its confluence into the Yukon River, near the hamlet of Carmacks, in the Klondike region of Yukon (Fig. 1). This section of river includes a reach with a well-developed meandering planform characterized by an ~15–20 m-wide channel. The river and its floodplain are found in the traditional and ancestral lands of the Little Salmon Carmacks First Nation. Here, we present the preliminary results of a geomorphic assessment of landscape change related to meander migration, including long-term analyses and a characterization of patterns of erosion and deposition related to a recent flood (June 2022) that resulted in widespread floodplain inundation upstream of Carmacks (Figs. 2 and 3). This study is part of a broader research effort aimed at investigating the morphodynamics and biogeochemistry of meandering rivers in the permafrost zone, and may serve as a template for the assessment of landscape change elsewhere in northern fluvial systems.

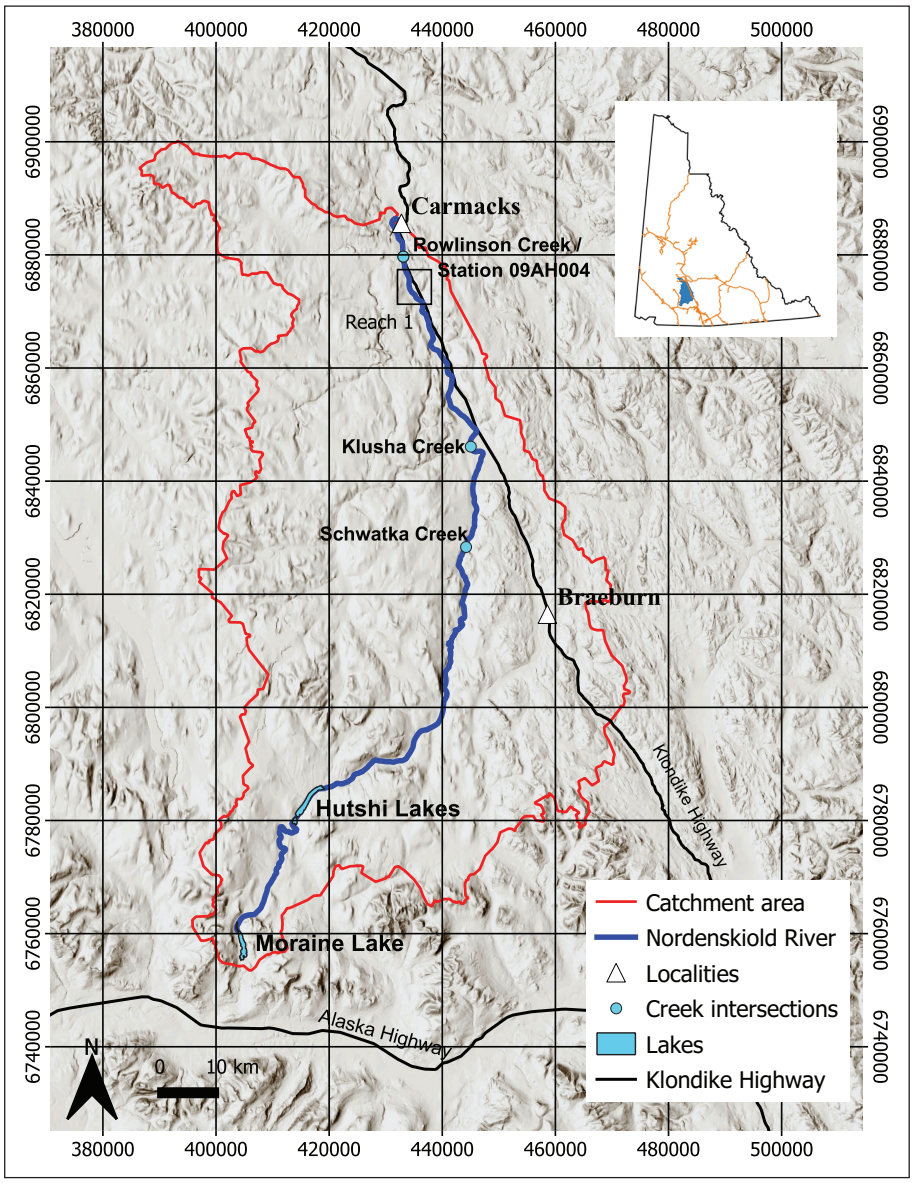

Figure 1. *Geographic sketch representing the Nordenskiold River's watershed (reported in blue in the inset; also includes Yukon highways, in orange, for geographic reference). Grid coordinates refer to metres in the WGS 84 UTM 8N projection. Reaches 2 and 3 are omitted for clarity.*

Regional setting

The Nordenskiold River flows through the Lewes plateau, in the northern Coast Mountain range of the Northern Cordillera (Mathews, 1986). The river originates from Moraine Lake at an elevation of 910 m (60.946° N, 136.760° W) and flows northward to eventually join the Yukon River at Carmacks at an elevation of 519 m (62.102° N, 136.301° W). The Nordenskiold River is approximately 185 km in length, draining a basin of ~6620 km^2. The river is characterized by a predominantly meandering planform with minor straight reaches, and runs northward through Hutshi Lakes (61.178° N, 136.566° W), joining Schwatka Creek (61.582° N, 136.053° W), Klusha Creek (61.735° N, 136.030° W) and Rowlinson Creek (62.044° N, 136.279° W). The average gradient of the river is 2.11‰, although it locally steepens downstream of the confluence with Rowlinson Creek, where it reaches an average gradient of 4.64‰. In this final, steeper reach, the river flows by a gap between glaciofluvial terraces on its hydrographic right-hand side that has previously been identified as a site of possible avulsion (*i.e.*, sudden channel relocation towards a steeper, shorter corridor) by Cronmiller et *al.* (2020). Such potential avulsion would pose significant flooding hazard to the community of Carmacks.

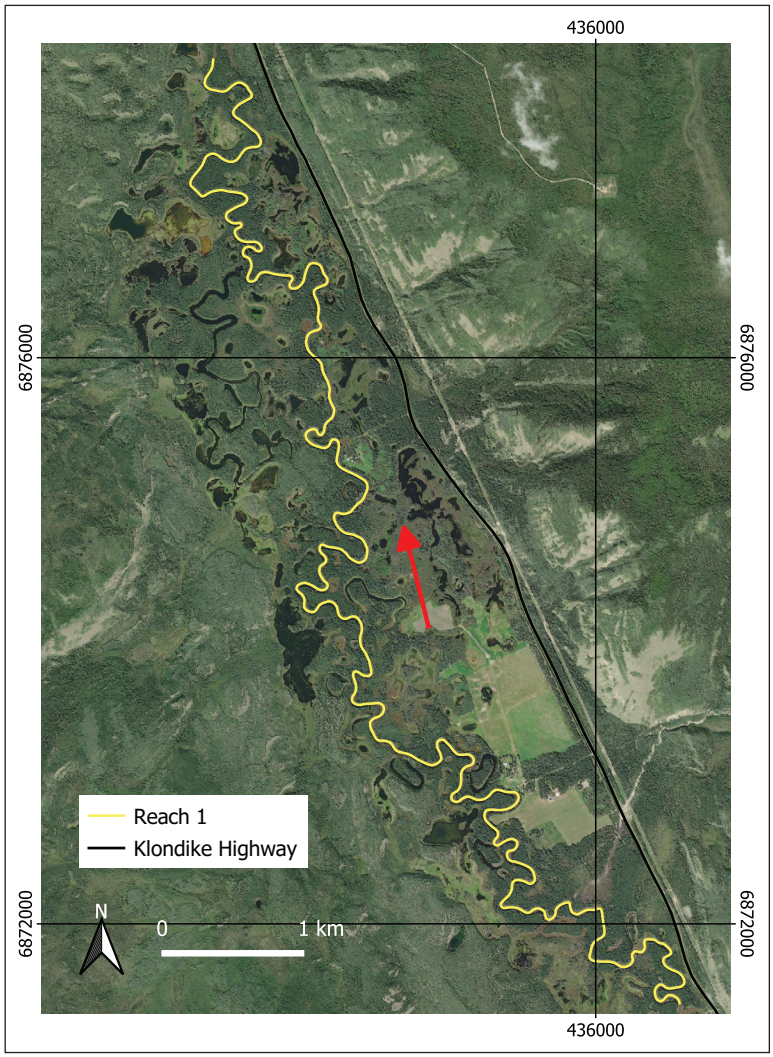

Figure 2. *Satellite view of the Nordenskiold River's reach 1. Grid coordinates refer to metres in the WGS 84 UTM 8N projection. Arrow indicates direction of flow.*

The river watershed is underlain by the Yukon-Tanana terrane, which includes metamorphosed and deformed siliciclastic and volcanic rocks of Late Proterozoic to Devonian age (Nelson and Colpron, 2007). The area has undergone a number of glaciations, which sculpted the hills around Carmacks, and led to the deposition of a mantle of till over uplands in the area (Cronmiller et *al.*, 2020). Large glaciofluvial outwash plains were formed at the terminus of ice sheets and were subsequently eroded by incising drainage networks as the ice withdrew, leaving behind a variable topography consisting of terraces with small kettle depressions and large, chaotic, hummocky ice stagnation complexes. The latter record stationary ice that filled a large portion of the Nordenskiold and Yukon rivers' floodplains at the end of the McConnell Glaciation (Marine Isotope Stage 2; Cronmiller et al., 2020). During glacial recession, strong katabatic winds coming off the ice sheets mobilized fine sediment in large volumes and deposited veneers of loess and less commonly dune ridges over much of the landscape. Presently, fluvial processes and anthropogenic activities such as mining and road building modify the landscape. A few areas around Carmacks are also undergoing localized landslides due to the occurrence of fluvial undercutting, locally mediated by permafrost-thaw processes (Cronmiller et *al.*, 2020). The study area is in the extensive discontinuous permafrost zone (Heginbottom et *al.*, 1995; Bonnaventure and Lewkowicz, 2012). Permafrost is most common on north-facing slopes and in valley bottoms, particularly in areas where thick organic materials preserve cold ground temperatures.

The Nordenskiold River has been included in the Tsâwnjik Chu Habitat Protection Area (Government of Yukon, 2010). Most of the wetlands surrounding the river have shallow open water, encircled by sedge zones and vast beds of submergent vegetation. Some of the wetlands have more complex sedge-grass communities, flooded willow stands, spike rush beds and horsetail scouring rush beds. The treed areas surrounding the wetland are composed mainly of aspen and white spruce, with some pockets of black spruce (Government of Yukon, 2010). The wetlands of the Nordenskiold River offer a habitat for breeding ducks, swans and geese as they rest during the fall migration. The channel provides spawning habitat for salmon, and 11 species of fish have been recorded in the watershed: chinook and chum salmon, lake trout, Arctic grayling, round and lake whitefish, longnose sucker, burbot, northern pike, Arctic lamprey, and slimy sculpin (Government of Yukon, 2010).

Figure 3. *Satellite view of the Nordenskiold River's reach 2. Grid coordinates refer to metres in the WGS 84 UTM 8N projection.*

Environment and Climate Change Canada operate a weather station in Carmacks (Station 1509; https://climate.weather.gc.ca/). The climate in this area is characterized by long, comfortable summers and frigid, snowy winters. Between the years of 1961 and 1990, daily mean temperatures ranged from -28.6°C (January) to 14.8°C (July), and average precipitation ranged from 6.8 mm per month (April) to 55.1 mm per month (July). A gauging station operated by Water Survey of Canada (Station 09AH004; https://wateroffice.ec.gc.ca/) is found immediately downstream of the Rowlinson Creek confluence (62.051° N, 136.280° W), and has been recording data since 1983. Minimum discharge levels (~3 $m^3 s^{-1}$) occur in the colder months (December–February), with an all-time estimated low of 1.19 m^3/s in January 1999. Maximum discharge levels occur during snowmelt, with a historical daily average maximum of 244 $m^3 s^{-1}$ in May 1983 (Fig. 4). A more detailed hydrological characterization is presented below.

Materials and methods

This study is based on the collection of photogrammetric and observational data of fluvial forms and processes from freely distributed satellite imagery and aerial photos, proprietary orthomosaics and digital surface models, and both planform and oblique imagery collected with unmanned aerial vehicles (UAVs). Freely distributed satellite imagery was accessed from the archives of Google™ Earth and ESRI™ World Imagery, with spatial resolution of 1.2 metres. Air photo 19, from flight A17344 (dated 1961) was retrieved from the Government of Yukon public archives. Drone North produced a proprietary orthomosaic and digital surface model for a subset of the study area with spatial resolutions of, respectively, 3.3 and 6.6 cm (Drone North, 2022). The collected drone imagery is characterized by variable spatial resolution based on flight attitude and altitude, notably with a set of planform images collected just upstream of Carmacks with centre-image ground resolution of ~10 cm.

Morphometric observations on meander geometry were first collected in order to provide a baseline data set to allow a comparison between the Nordenskiold River and meandering rivers elsewhere within and outside the permafrost zone. We consider individual meander bends with a sinuosity index (defined as the ratio between along-channel length and linear distance) higher than 1.2. The imagery was also employed to manually digitize polylines representing the

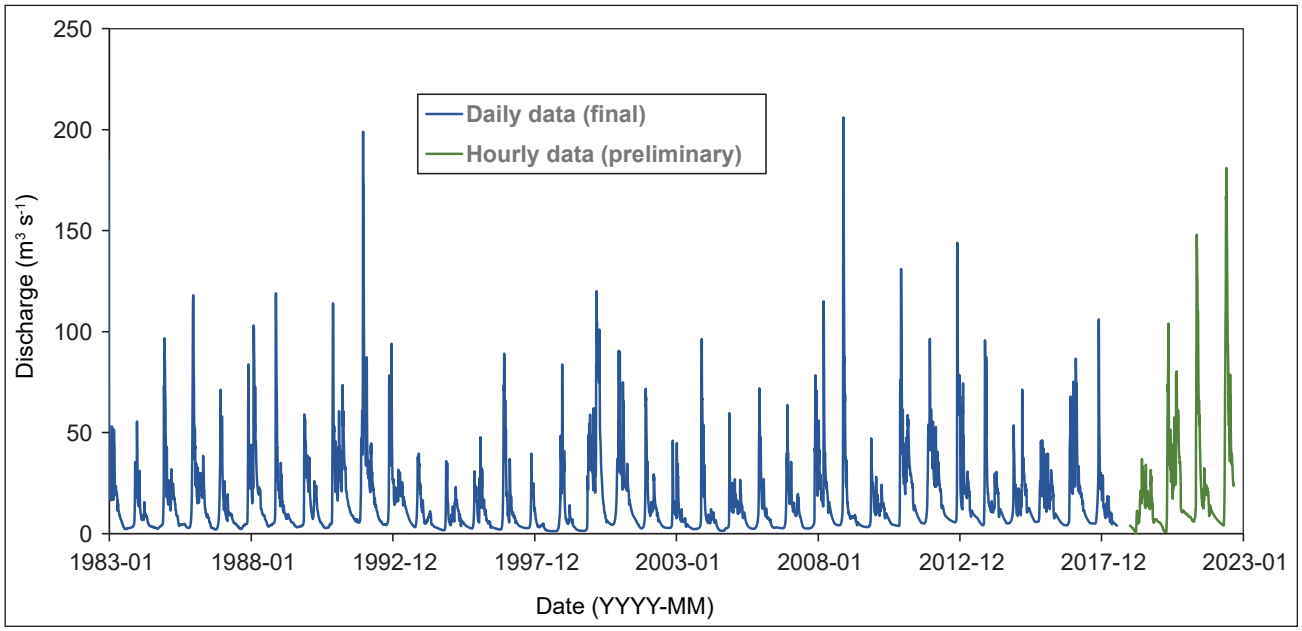

Figure 4. *Hydrograph of daily discharge data at Station 09AH004.*

position of the hydrographic left and right-hand banks of the main channel of the Nordenskiold River at different dates over three selected reaches that together capture the river's geomorphic variability. The comparison of digitized products at different times allowed for the characterization of landscape change associated with fluvial processes such as bank erosion, bar deposition and channel overspilling.

Reach 1 is defined from 61.971° N, 136.209° W to 62.029° N, 136.274° W, covering an along-channel distance of ~16 km. This reach is located about 2 km along-channel upstream of the confluence between the Nordenskiold River and Rowlinson Creek, and displays a classic high-sinuosity meandering channel planform. This reach shows evidence of widespread degrading (thermokarst) permafrost throughout its length. Bank lines along this reach were digitized from imagery dated September 24, 2008 and August 5, 2017. Two boreholes were drilled about 14 km upstream of reach 1 (61.857° N, 136.110° W). The boreholes are located about 50 m apart, and sample both an inner and outer bank along two consecutive meanders.

Reach 1 and 2 are separated by a ~3.5 km-long channel segment with straight planform, where the river is narrowly confined within a valley sided by glaciofluvial terraces. Reach 2 is defined from 62.060° N, 136.280° W to 62.102° N, 136.301° W, over an along-channel distance of ~8 km. This reach of the Nordenskiold River is immediately upstream of the Yukon River and displays a wandering to meandering channel planform. Bank lines along this reach were digitized from imagery dated 1961 (day and month unspecified and, based on lack of snow on the ground and low flow, arbitrarily set to August 1) and August 5, 2017. Reach 3 is developed along a subset of reach 2, from 62.073° N, 136.298° W to 62.082° N, 136.303° W, over an along-channel distance of ~2 km. This reach represents a sensitive area near active roadworks and town infrastructures and dwellings. Bank lines along this reach were digitized from imagery dated August 5, 2017 and October 11, 2022, which predate and postpone the June 2022 flood, respectively.

All bank lines and derived data products were digitized and processed in the QGIS environment as shapefiles. Specifically, pairs of hydrographic left and right-hand bank lines were used to construct channel centrelines through a process of skeletonization, using an open-access toolbox developed in the *R* programming language and chained within QGIS (http://mlt.github.io/QGIS-Processing-tools/tags/dtw.html). Skeletonization returns a centreline where each node is spaced from others at a defined interval (in this study, we employed a 10 m spacing that captures the changing curvature of the meandering channel). Centrelines representative of different dates were then compared, using the same toolbox, through dynamic time warping – an algorithm that compares polylines from different dates and stretches or compresses them to produce migration pathways at discrete spatial intervals (Giorgino, 2009). In other words, dynamic time warping generates lines representing migration pathways along the river course at discrete spatial intervals (here corresponding to the node spacing along the centrelines). Dynamic time warping was also employed to obtain channel-width data by comparing the hydrographic left and right-hand bank lines representative of a given date. Only channel bends that underwent planform change through actual lateral migration were included in this analysis, whereas channel sections that underwent cutoff, braiding, or relocation were manually removed. This analytical approach allows us to plot data such as channel width, curvature, and migration rate, as a function of along-channel distance. Finally, photogrammetric data were corroborated by observational data collected in the field during two visits, one in June and one in October 2022 (at high and low flow conditions). All field and photogrammetric observations were also compared against discharge data.

Preliminary results and discussion

Hydrology

Discharge data from the Nordenskiold River spanning from 1983 to 2018 were analyzed. Over this 35-year interval, the highest discharge typically occurred in relation to late spring/early summer freshet, *i.e.*, in the window between mid-May to late June, with a lowest maximum peak of 38.1 $m^3 s^{-1}$ in 1995, a maximum peak of 244 $m^3 s^{-1}$ in 1983, and a mean from all annual peaks of 102 $m^3 s^{-1}$. We constructed a record of discharge data plotted as a function of exceedance recurrence interval (Fig. 5), fitted with a Log-Pearson III regression. Peak annual discharges in the range of 50 to 125 $m^3 s^{-1}$ have return periodicities of 1 to 5 years, which can be used as a first order estimate for the range of bankfull discharge (*i.e.*, the typical formative discharge of a river, above which water overspill onto the adjoining floodplain takes place; Wolman and Miller, 1960). The plot in Figure 5 also shows the occurrence of three events with discharge >200 $m^3 s^{-1}$, which, considering the data set at hand, correspond to exceptional floods with return interval of 15 to at least 40 years. Peak-annual-discharge data show a log-normal distribution with respect to exceedance recurrence intervals, as observed in rivers elsewhere across a range of biogeomorphic regimes (Ielpi *et al.*, 2020; Kuras *et al.*, 2021).

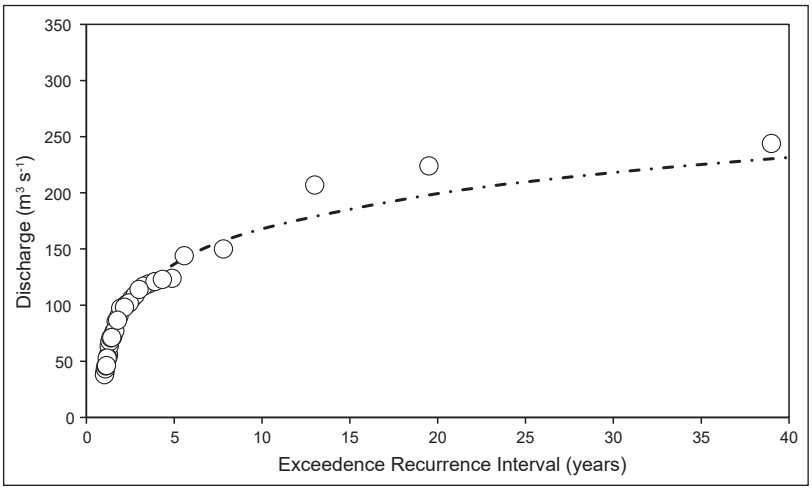

Figure 5. *Peak annual discharge from Station 09AH004 plotted as a function of exceedance recurrence interval. A Log-Pearson III fit is reported for reference.*

In the late spring and early summer of 2022, the Nordenskiold River experienced higher flood levels than average. Preliminary data (that is, not yet been subject to full quality assessment and control by the Water Survey of Canada) show that discharge began increasing on April 24, starting at 4 $m^3 s^{-1}$ and eventually reaching a peak of 186 $m^3 s^{-1}$ on May 28 (Fig. 6). Discharge levels then steadily decreased, with the exception of two secondary peaks on July 1 and 15 related to significant precipitation impacting the watershed. Discharge plateaued back to low-flow stages on August 6. According to the data compiled in Figure 5, the spring 2022 flood categorizes as a discharge event with a return interval of about 10 years. This flood lead to widespread overspill onto the river's floodplain (Fig. 7). Overspilling affected mostly thermokarst lowland areas located within 2 km of the active channel, especially along reach 1. Notwithstanding higher-than-usual water levels, no significant overspill took place along reach 2, likely due to the channel being more confined along its final, steeper section upstream of the Yukon River confluence. This observation suggests that, at least considering floods with ~10 years of recurrence interval, no impending risk of channel avulsion occurs at the gap between glaciofluvial terraces near Carmacks (*cf.*, Cronmiller *et al.*, 2020).

Morphodynamics

Permafrost was intersected in the two boreholes upstream of reach 1 at depths of about 0.7 m. Frost probing in the area likewise found a highly variable active layer thickness ranging from 0.7 to >1.3 m. No evidence of permafrost was observed along reaches 2 and 3, though it may be present in portions of the floodplain distal to the active channel and topographically shielded from insolation. Fifty-four meanders were measured along reach 1 (Fig. 8), yielding a median ±1σ range in channel length of 287^{+238}_{-122} m (where σ defines the deviation between of the 16th and 84th percentiles in a distribution from the median). Meander diameter data (*i.e.*, the along-valley distance between consecutive bend inflection points) along reach 1 yielded a median ±1σ range of 111^{+80}_{-51} m. Accordingly, the sinuosity index data for reach 1 yielded a median ±1σ range of $2.44^{+1.15}_{-0.68}$. Twelve meanders were measured along the shorter reach 2 (Fig. 8). These meanders produce a median ±1σ channel length of 616^{+237}_{-112} m, a median ±1σ diameter of 319^{+115}_{-112} m, and a median of ±1σ sinuosity index of $2.06\pm^{+1.08}_{-0.64}$. These preliminary results show that the Nordenskiold River has similar scalar relationships as rivers elsewhere both within and outside the permafrost zone (Williams, 1986; Ielpi *et al.*, 2021; Whitney, 2022). More detailed analyses will investigate possible departures between the morphodynamics of the Nordenskiold and other rivers in diverse bioclimatic regions.

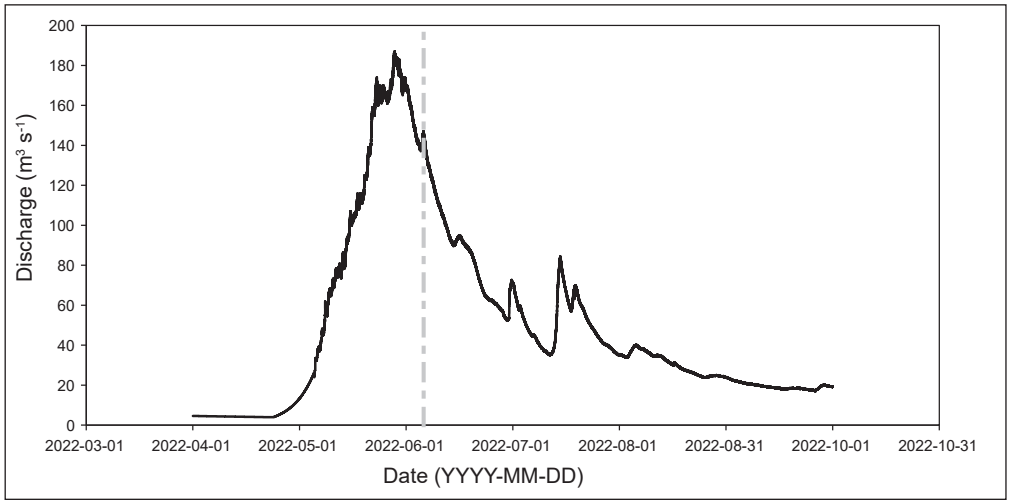

Figure 6. *Hydrograph of preliminary instantaneous discharge data at Station 09AH004, detailing the May–June 2022 flood. The dashed grey line indicates the day of the field visit and photograph in Figure 7.*

Figure 7. *Oblique aerial photograph depicting the Nordenskiold River (foreground) and adjoining inundated floodplain near the upstream-most part of reach 1. Photograph taken in early June 2022; arrow depicts flow direction in mainstem channel. The thermokarst ponds, as depicted here as flooded lowlands siding the main channel, are ubiquitous in Reach 1.*

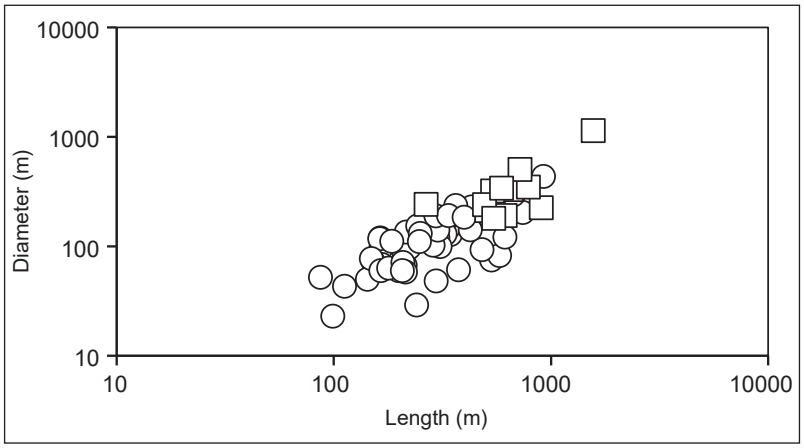

Figure 8. *Log-log plot of morphometric data on meander-size distribution for the Nordenskiold River along reaches 1 and 2. Length and diameter indicate, respectively, along-channel and along-valley distances between bend-inflection points.*

Data on migration rate, channel width and bend curvature obtained through dynamic time warping are reported in Figures 9 through 14. Along reach 1, absolute curvature has a median ±1σ range of $1.1^{+1.4}_{-0.8} \times 10^{-2}\,m^{-1}$ (Fig. 9), channel width a median ±1σ range of $23.6^{+4.3}_{-3.2}$ m (Fig. 10), and migration rate averaged from 2008 to 2017 a median ±1σ range of $0.45^{+0.16}_{-0.21}$ m yr^{-1} (Fig. 11). Along this reach, both bend curvature, channel width and migration rate show decreasing trends downstream (Figs. 9–11). Whereas the decrease in bend curvature is minimal, channel width ranges from about 15 to 45 m in the upstream-most 3 km and from about 15 to 25 m in the downstream-most 2 km (*i.e.*, a relative decrease of about ⅓; Fig. 10). Migration rates also show a decrease of comparable magnitude, ranging from local maxima of 1.4 m yr^{1} in the upstream-most tract to 0.7 m yr^{1} in the downstream-most tract (Fig. 11).

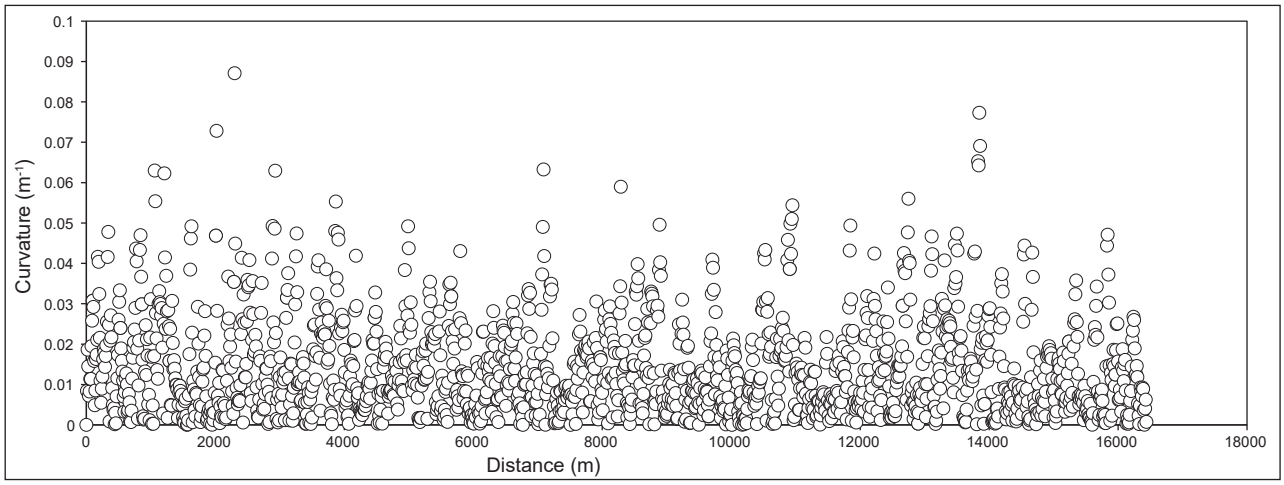

Figure 9. *Bend curvature along reach 1 plotted as a function of downstream distance.*

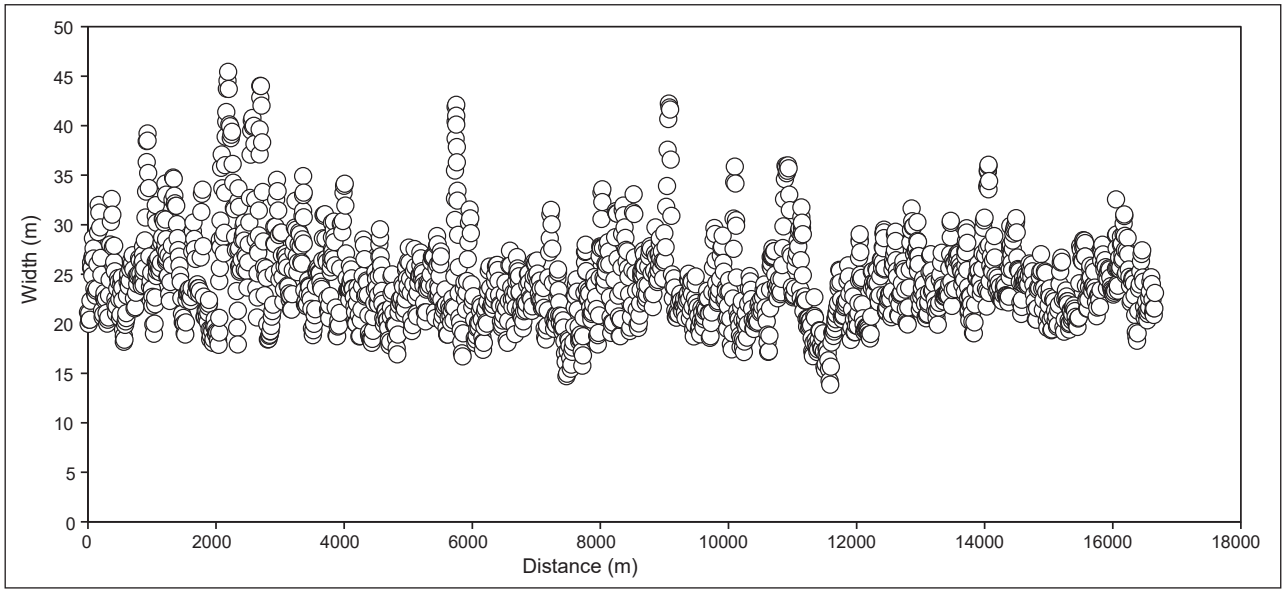

Figure 10. *Channel width along reach 1 plotted as a function of downstream distance.*

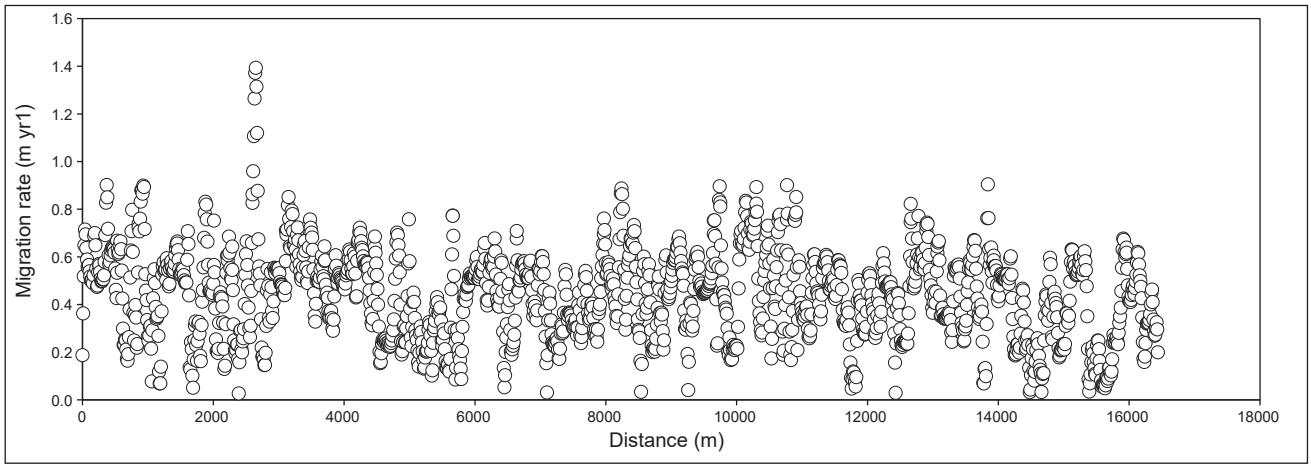

Figure 11. *Migration rate along reach 1 plotted as a function of downstream distance.*

Along reach 2, absolute curvature has a median ±1σ range of $7.0^{+1.2}_{-0.05} \times 10^{-2}\,m^{-1}$ (Fig. 12), channel width a median ±1σ range of $35.7^{+25.5}_{-10.7}$ m (Fig. 13), and migration rate averaged from 1961 to 2017 a median ±1σ range of $0.22^{+0.59}_{-0.16}$ m yr $^{-1}$ (Fig. 14). These parameters likewise display slightly decreasing trends downstream, although with sharper relative variations than in reach 1 (Figs. 12–14). The morphodynamic data presented through dynamic time warping show that, overall, the Nordenskiold River is characterized by similar curvature and migration rate in relation to channel width to other rivers found in different bioclimatic regions (Constantine *et al.*, 2014; Sylvester *et al.*, 2019; Ielpi and Lapôtre, 2020, 2022). The above suggests that the presence of discontinuous permafrost in the river's alluvial plain does not noticeably affect parameters like bank strength, such that the river's morphodynamic characteristics are similar to those of other watercourses outside the permafrost zone. That being said, the marked downstream decrease in channel width and migration observed along reach 1 may be related to changes in stream power related to, hydrologic loss of the channel towards the floodplain's aquifer.

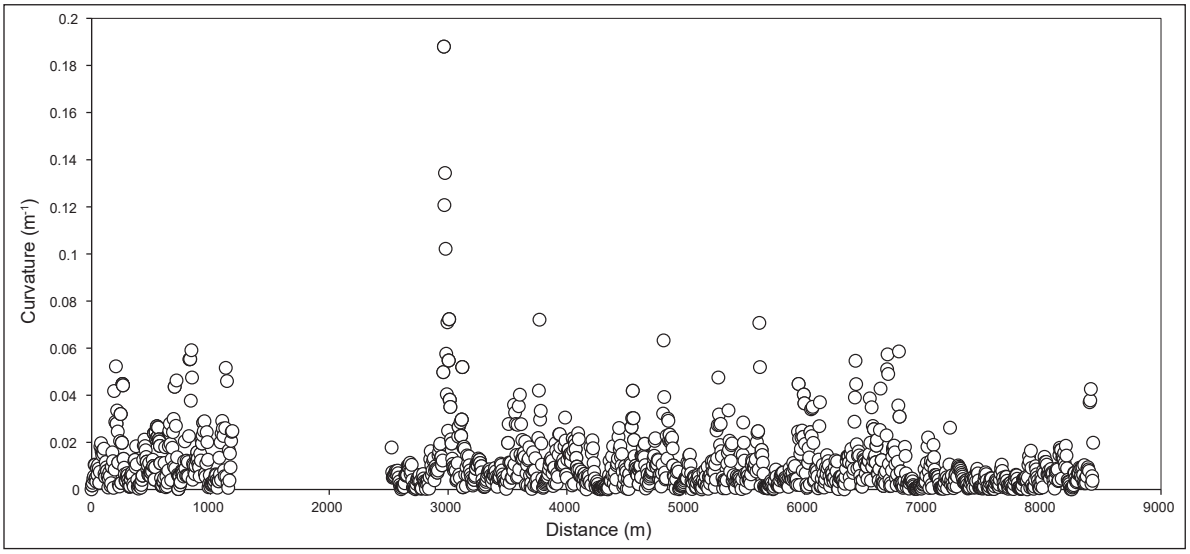

Figure 12. *Bend curvature along reach 2 plotted as a function of downstream distance. Omitted values are along a reach that underwent chute cutoff and that were not considered in the dynamic time warping.*

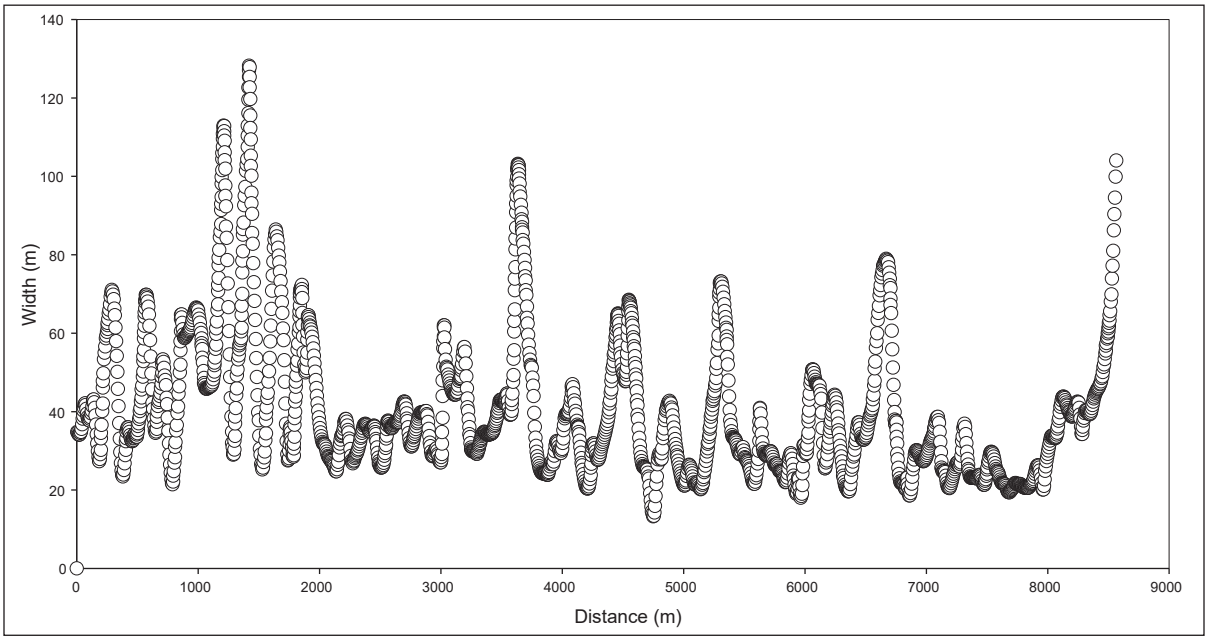

Figure 13. *Channel width along reach 2 plotted as a function of downstream distance.*

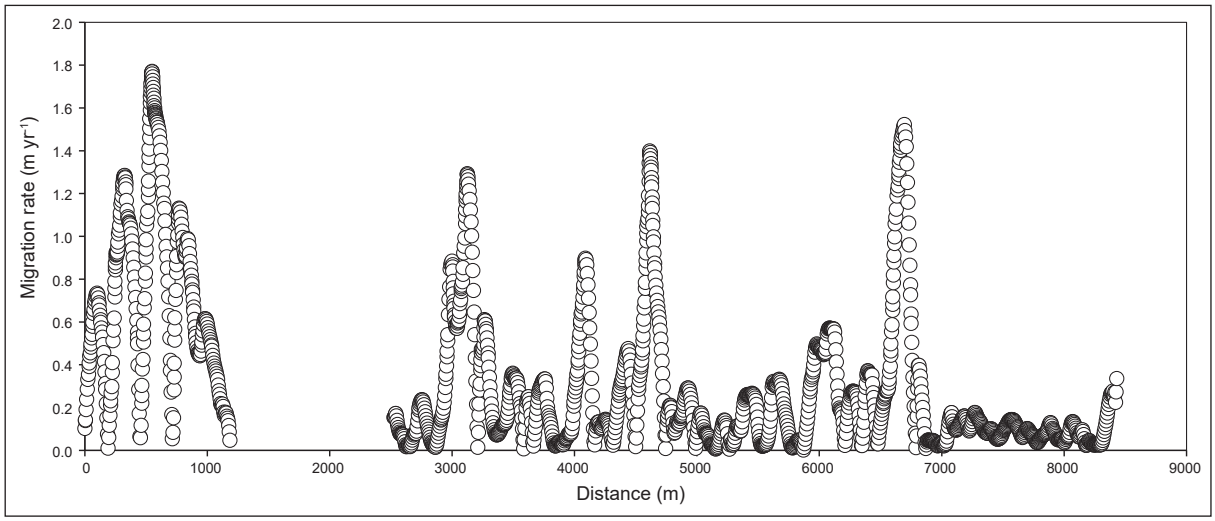

Figure 14. *Migration rate along reach 2 plotted as a function of downstream distance. Omitted values are along a reach that underwent chute cutoff and were not considered in the dynamic time warping.*

Results above inform potential hazards related to fluvial processes near Carmacks — hazard being broadly defined as risk in relation to a phenomenon that can potentially lead to harm or damage to lives and existing properties and infrastructures. Reach 1 has little potential hazard related to channel migration since bank erosion is not likely to impact infrastructures (with the notable exception of locations where the channel's outer bank impinges directly on the Klondike Highway, e.g., at 61.970° N, 136.205° W). The hazard is however greater along reach 2 (and its subset, reach 3) in response to floods with above-decadal recurrence interval based on migration rates and pathways, but also on the occurrence of infrastructures and dwellings (Fig. 15). That being said the potential for a significant avulsion of the Nordenskiold River at Carmacks (as discussed by Cronmiller *et al.*, 2020) is deemed low, considering the patterns of migration of the channel and its confined nature immediately upstream of the Yukon River confluence.

Conclusions

This report presented the preliminary results of a geomorphic survey focused on Tsā̃lnjik Chú (Nordenskiold River) near Carmacks, in the southern Klondike region of Yukon. Geomorphic assessments were aimed at acquiring baseline data on the morphometry and migration rate of the river in relation to hydrographic stages, including planform change in the aftermath of a ~10-year recurrence flood that took place in the spring of 2022. This report is part of a larger project focused on understanding the morphodynamics and biogeochemistry of meandering rivers in the permafrost zone. We employed hydrological analysis, photogrammetric measurements, borehole drilling, and algorithms such as dynamic time warping to investigate river-landscape change. Preliminary results indicate that the river plain is underlain by discontinuous permafrost, with thaw-front depths as shallow as ~0.7 m, and that the river is characterized by similar relationships between channel size, curvature and migration

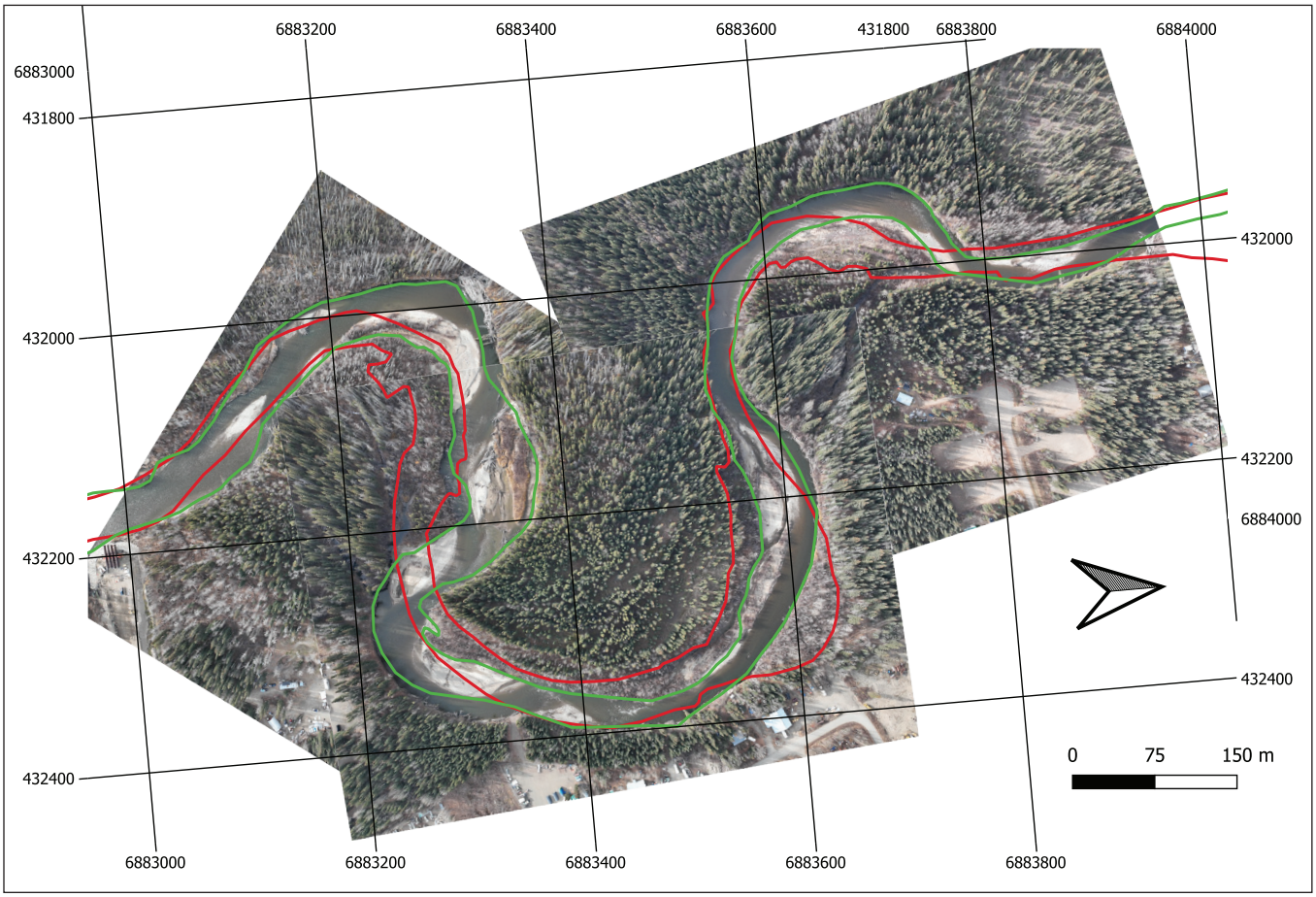

Figure 15. *Collage of georeferenced planview UAV imagery from October 2022 of reach 3 (flow to the right), with channel banks from 1961 and 2017 reported, respectively, in red and green. Note locally ongoing erosion along hydrographic right banks (bottom of the image), in the vicinity of infrastructures and dwellings. Grid coordinates refer to metres in the WGS 84 UTM 8N projection.*

rate to other rivers located outsized the permafrost zones. Channel migration and flooding related to ~10+ year-recurrence floods have little predicted impact on upstream meandering reaches of the river located several kilometres away from Carmacks, whereas channel migration and overspill in the terminal reach immediately upstream of the confluence with the Yukon River has the potential to affect infrastructures and dwellings. That being said, an analysis of the river profile suggests that avulsion events in the lowermost river course (e.g., along Carmacks) are unlikely. These results will inform future work: (i) an investigation of patterns of organic-carbon budgeting in the river's floodplain thanks to recently acquired soil samples; and (ii) a fuller characterization of ground-temperature profiles in relation to ice content and, more broadly, permafrost distribution along the two boreholes drilled in the river's floodplain.

Acknowledgements

Stefan Gronsdahl is acknowledged for reviewing the manuscript, and for helping with the Log-Pearson III fit of flood recurrence intervals. This work is part of the BSc Honours thesis of the lead author. CH and AI acknowledge financial support from the Yukon Geological Survey, Polar Knowledge Canada's Northern Scientific Training Program, and the Natural Sciences and Engineering Research Council of Canada's Discovery Grant Program.

References

Bonnaventure, P.P. and Lewkowicz, A.G., 2012. Permafrost probability modeling above and below treeline, Yukon, Canada. Cold Regions Science and Technology, vol. 79-80, p. 92–106, https://doi.org/10.1016/j.coldregions.2012.03.004.

Constantine, J.A. and Dunne, T., 2008. Meander cutoff and the controls on the production of oxbow lakes. Geology, vol. 36, p. 23–26, doi:10.1130/G24130A.1.

Constantine, J.A., Dunne, T., Ahmed, J., Legleiter, C. and Lazarus, E.D., 2014. Sediment supply as a driver of river meandering and floodplain evolution in the Amazon Basin. Nature Geoscience, vol. 7, p. 899–903, doi:10.1038/ngeo2282.

Cronmiller, D.C., McParland, D.J., Goguen, K.M. and Mckillop, R.J., 2020. Carmacks surficial geology and community hazard susceptibility mapping. Yukon Geological Survey, Miscellaneous Report 20, 16 p.

Donovan, M., Belmont, P. and Sylvester, Z., 2021. Evaluating the relationship between meander-bend curvature, sediment supply, and migration rates. Journal of Geophysical Research: Earth Surface, vol. 126, doi:10.1029/2020JF006058.

Drone North, 2022. Nordenskiold river project uav photogrammetry survey – October 2022, 15 p.

Gillet, N., Flato, G., Zhang, X., Derksen, C., Bonsal, B., Greenan, B., Bush, E., Shepherd, M., Peters, D. and Gilbert, D., 2019. Canada's Changing Climate Report. Government of Canada, 444 p., http://www.changingclimate.ca/CCCR2019.

Giorgino, T., 2009. Computing and Visualizing Dynamic Time Warping Alignments in R: The dtw Package. Journal of Statistical Software, vol. 31, p. 1–24, doi:10.18637/jss.v031.i07.

Government of Yukon, 2010. Tsâwnjik Chu Nordenskiold Habitat Protection Area Management Plan. Prepared by the Nordenskiold Steering Committee and Yukon Department of Environment, 28 p.

Heginbottom, J.A., Dubreuil, M.A. and Harker, P.A., 1995. Canada, Permafrost. *In:* National Atlas of Canada, Natural Resources Canada, Geomatics Canada, MCR Series no. 4177 (5th Edition), 1 sheet.

Horton, A.J., Constantine, J.A., Hales, T.C., Goossens, B., Bruford, M.W. and Lazarus, E.D., 2017. Modification of river meandering by tropical deforestation. Geology, vol. 45, p. 511–514, doi:10.1130/G38740.1.

Ielpi, A. and Lapôtre, M.G.A., 2020. A tenfold slowdown in river meander migration driven by plant life. Nature Geoscience, vol. 13, p. 82–86, doi:10.1038/s41561-019-0491-7.

Ielpi, A. and Lapôtre, M.G.A., 2022. Linking sediment flux to river migration in arid landscapes through mass balance. Journal of Sedimentary Research, vol. 92, p. 695–703, https://doi.org/10.2110/jsr.2022.118.

Ielpi, A., Lapôtre, M.G.A., Finotello, A. and Ghinassi, M., 2021. Planform-asymmetry and backwater effects on river-cutoff kinematics and clustering. Earth Surface Processes and Landforms, vol. 46, p. 357–370, doi:10.1002/esp.5029.

Ielpi, A., Lapôtre, M.G.A., Finotello, A., Ghinassi, M. and D'Alpaos, A., 2020. Channel mobility drives a diverse stratigraphic architecture in the dryland Mojave River (California, USA). Earth Surface Processes and Landforms, vol. 45, p. 1717–1731, doi:10.1002/esp.4841.

Jackson, R.G., 1976. Depositional Model of Point Bars in the Lower Wabash River. SEPM Journal of Sedimentary Research, vol. 46, doi:10.1306/212f6ff5-2b24-11d7-8648000102c1865d.

Kuras, P., Trubilowicz, J. and McLean, R., 2021. British Columbia Extreme Flood Project, Regional Flood Frequency Analysis – Technical development report and manual to complete a regional flood frequency analysis. Bulletin 2020-1-RFFA, doi: 10.13140/RG.2.2.29177.80480.

Lewis, G.W. and Lewin, J., 1983. Alluvial cutoffs in Wales and the Borderlands. *In:* Modern and ancient fluvial systems, J.D. Collinson and J. Lewin (eds), Wiley Online Library, p. 145–154, https://doi.org/10.1002/9781444303773.ch11.

Mason, J. and Mohrig, D., 2019. Differential bank migration and the maintenance of channel width in meandering river bends. Geology, vol. 47 p. 1136–1140, doi:10.1130/G46651.1/4836975/g46651.pdf.

Matthews, W.H., 1986. Physiographic map of the Canadian Cordillera. Geological Survey of Canada, Series Map 1701A, 1 sheet, doi:10.4095/122821.

Nanson, G.C., 1980. Point bar and floodplain formation of the meandering Beatton River, northeastern British Columbia, Canada. Sedimentology, vol. 27, p. 3–29, doi:10.1111/j.1365-3091.1980.tb01155.x.

Nanson, G.C. and Hickin, E.J., 1983. Channel Migration and Incision on the Beatton River. Journal of Hydraulic Engineering, vol. 109, p. 327–337, doi:10.1061/(asce)0733-9429(1983)109:3(327).

Nelson, J. and Colpron, M., 2007. Tectonics and metallogeny of the British Columbia, Yukon and Alaskan Cordillera, 1.8 Ga to the present. *In*: Mineral Deposits of Canada: A Synthesis of Major Deposit-Types, District Metallogeny, the Evolution of Geological Provinces, and Exploration Methods, W.D. Goodfellow (ed.), Geological Association of Canada, Special Publication No. 5, p. 755–791.

Sylvester, Z., Durkin, P. and Covault, J.A., 2019. High curvatures drive river meandering. Geology, vol. 47, p. 263–266, doi:10.1130/G45608.1.

Whitney, J., 2022. Geomorphic and carbon dynamics in a continuous permafrost floodplain: Blackstone River, Yukon, Canada. MSc thesis, Laurentian University, 100 p.

Williams, G.P., 1986. River meanders and channel size. Journal of Hydrology, vol. 88, p. 147–164.

Wolman, M.G. and Miller, J.P., 1960. Magnitude and Frequency of Forces in Geomorphic Processes. The Journal of Geology, vol. 68, p. 54–74, doi:10.1086/626637.